Active Noise Hybrid Time-Varying Control for Motorcycle Helmets

Rosa Castañé-Selga and Ricardo S. Sánchez Peña,

***Abstract*—Recent noise at work regulations in the EU (2003) have been established to prevent noise induced hearing loss (NIHL). This imposes better performance results to traditional feedback active noise control (ANC) in motorcycle helmets, which suffer from well known limitations. Here two new ideas are applied to this problem. First, an hybrid (feedforward/feedback) linear time invariant (LTI) controller is designed for a motorcycle helmet ANC, which improves the resulting attenuation. This is achieved by adding an extra pair of microphones which measure the external noise that is then used as the feedforward input signal. In addition and to increase even more the resulting performance, the air velocity is measured in real-time and used as the parameter which schedules a linear parameter varying (LPV) feedback (FB) controller. This is combined with the previous feedforward (FF) controller, resulting in a time-varying hybrid controller. Both hybrid, LTI and LPV controllers are designed using linear matrix inequality (LMI)-based optimization. Two experiments have been carried out to measure the relation between external noise spectra and velocity: a wind tunnel test and a freeway ride experience. The resulting controllers are tested in a simulation which uses actual data obtained from the freeway experiment. The resulting attenuations in this motivating study seem promising for future controller tests to be performed in real-time, with the adequate hardware.**

I. Introduction

ACTIVE noise cancellation (ANC) in motorcycle helmets has received special attention in the last few years due to the recent European legislation of noise in work environments [1]. This legislation, establishes a maximum level of noise that workers can suffer during a regular working day [$<$ 87 dB (A)] in order to prevent noise induced hearing loss (NIHL). The problem is that these laws are very difficult to fulfill with existing technology. In particular, occupational motorcyclists such as policemen, delivery employees, sportsmen, are in risk of NIHL. Several medical studies [2]–[5] point out that, with the inner helmet noise levels and the typical driving patterns, the percentage of exposed population that will suffer a hearing loss of 30 dB or more ranges from 40 for professional racers, 36% for paramedics and 6% for driving instructors.

Nowadays, there are many noise reduction techniques, for example, the use of earplugs can be very practical but it does not provide a good attenuation for low frequency noise and also complicates the use of radio communication equipment. The use of a proprietary neck seals has been demonstrated to reduce up to 4 dB at 120 Km/h but it is very difficult to fit in many situations and the wind can pull it out of the helmet. In 1997 [6] the use of noise cancelling earphones in full coverage style helmets was patented and proved that the use of ANC techniques does not present any of these disadvantages. Nevertheless, the traditional ANC used in helmets is based only on feedback, whose limitations have been extensively studied [7]–[9] and produces low performance in general.

ANC is a well documented area of research [10], [11] that presents many particularities, depending on the application. There are many works on ANC in rooms, headphones or tubes as documented in [8], [12], and [13] but very few works on active noise control in helmets. In [14], an adaptive feedback in helmets and headsets used by the Finish Air Force pilots is presented and some interesting aspects on the implementation are treated. In [15]–[17] a feedback ANC system for earphone applications is introduced and in [18] the ideal position of the error microphone was studied and determined experimentally. On the other hand, there are a few more works concerned on the health consequences (NIHL) of the noise in occupational motorcyclists [3], [5].

All the works on ANC in helmets are based on a feedback scheme which suffers well known limitations and have in general low performance. Feedforward (FF) controllers instead are not subject to the typical performance limitations of the feedback loop, but need to guarantee stability and robustness. The two novelties of our approach are: the use of a feedforward controller and the real-time measurement of the air velocity, in order to increase the controller performance. This leads to the design of a two-degree-of-freedom (2DOF) hybrid[1] control structure, with both a feedback and a feedforward signal (see also [19]). The feedback signal is the actual noise in the ear of the motorcyclist sensed by a coupled set of microphones. The feedforward variable is the noise in a different part of the helmet, where the dominant external noise source appears. Both actuate over the driver ears by means of a set of matched speakers. The LTI FF control is designed based on an LMI-based recent methodology in [20]. Another option could be the use of an adaptive

This research was supported by ICREA and CICYT Project DPI2005–04722 and DPI2008-0403.

R. Castañé-Selga is with the Technische Universität München, Munich 85748, Germany.

R. S. Sánchez Peña is with the CONICET and the Buenos Aires Institute of Technology (ITBA), (C1106ACD) Buenos Aires, Argentina (e-mail: rsanchez@itba.edu.ar).

[1]Here the terminology *hybrid* refers to the FB/FF combination of controllers. It should not be confused with similar terminology used in the control area *jargon* which describes the combination of discrete and continuous time systems.

identification/cancellation scheme, which has been extensively used in other applications of ANC. One of the main problems is its stability [21], due to the fact that although it is open loop, it has a nonlinear closed loop structure. Here, a comparison between several adaptive procedures (RLS, LMS, normalized LMS, sign-sign LMS, sign-error LMS) and LTI FF algorithms has been performed, but a thorough comparison between both methodologies will be the object of future research.

The feedback (FB) controller has been designed based on two different approaches: an LTI and an LPV model of the helmet, the latter scheduled by the air velocity. In the first case, a traditional $\mathcal{H}_\infty$ optimal controller is designed which guarantees stability and robustness against helmet, sensor and actuator model uncertainties [22]–[24]. In the second case, if the external noise spectrum variation with velocity is exploited, a linear parameter varying (LPV) optimal controller can be applied which schedules an optimized performance design weight, and therefore improves the attenuation with respect to the LTI case.

Here, to compute the relation between the helmet inner noise and the motorcycle-air relative velocity, two experiments have been performed. The first one in a wind tunnel considering the velocity/noise relation as a parameter varying model. The other experiment was performed in the actual freeway with the helmet mounted on a car's roof. The resulting experimental database from this last experiment has been used as the actual feedforward signal to test both controllers.

This paper is organized as follows. Section II presents the problem formulation and the FB/FF framework for controller design. Section III presents both experiments performed to obtain the time variation of the noise spectrum with the motorcycle-air relative velocity: in the wind tunnel and in the freeway. Section IV present the hybrid controller designs for the time invariant and the time varying cases as well as the results. Final conclusions and comments on future work to be done end this paper in Section V.

II. Problem Formulation

It is clear that, when possible, FF control may significantly improve performance in active noise cancellation [13], [19]. In addition, air velocity seems to be a key variable in ANC for motorcycle helmets. The proposed hybrid ANC strategy measures the actual noise in the ear with a pair of omnidirectional matched microphones, the external noise entering the helmet with another pair of reference microphones, and the relative motorcycle-air velocity with an anemometer or pitot tube. Some basic characteristics of the system need to be determined to asses the objective.

- ***Dominant Noise Source:*** To establish the correct location of the reference microphones, the dominant noise source in the helmet has to be established. Several works [5], [25] state that above 60 km/h the aerodynamic noise caused by the airflow around the helmet and the driver exceeds the noise generated by the motorcycle itself. So, it will be important to study how this aeroacoustic noise is generated in order to know where to measure it.
- ***Control Structure:*** According to the literature and the available variables, the best control structure and the best control design have to be chosen. This step is essential in order to obtain the best performance while robust stability is guaranteed. It is well known that different control structures imply different limitations on the performance/robustness that can be achieved [9], [13], [26]. In addition, time invariant and/or time varying solutions should be considered.
- ***Required Attenuation:*** There are several works that determine which is the range of noise levels that motorcyclists suffer [4], [5], these being between 75 and 107 dB(A). As the European legislation of noise in work [1] establishes a maximum level of 87 dB(A), a 20 dB attenuation is therefore needed.
- ***Bandwidth (BW):*** The frequencies that generate the highest levels of noise have to be determined in order to be attenuated. The range of human hearing falls roughly within the range of sound waves with frequencies between 20 Hz and 20 kHz, but in addition the useful BW should be reduced to a much smaller set of frequencies where the most disturbing effects on the ear are produced. Moreover, this *tuning* of the effective BW should be made at different velocities if a high attenuation is required, i.e., a velocity (and time) dependent design.

A. Dominant Noise Source

There are several studies concerned with the definition of the noise sources in motorcycle helmets [3], [5], [25]. The engine noise is an important noise source for low velocities ($<$ 60 km/h), but as the velocity increases, the aerodynamic noise around the driver clearly becomes the dominant noise source.

When the aeroacoustics of the helmet is analyzed the mechanisms that generate aerodynamic noise [see Fig. 1(b)] are found to be the following: 1) aspiration ("leak") noise in the visor; 2) protuberance noise in the base of the helmet and the driver's neck and shoulders; 3) cavity flow noise between the neck and cheeks of the driver, and the helmet; 4) flow separation and reattachment noise; and 5) wake noise. All works in the literature agree that the first and the second noise sources become dominant when the velocity of the motorcycle is higher than 60–70 km/h. Several passive solutions have been proposed in order to reduce it, which have achieved attenuations between -5 and -8 dB. In [3] and [25] there are unequivocal evidences that this turbulence generates noise that increases logarithmically with speed and up to very high levels, e.g., 110 dB(A) at 158 km/h. These levels seem relatively constant regardless of the choice of helmet, motorcycle, or seating position.

None of these works show any information about the spectrum of this noise for a certain velocity and which are the most disturbing frequencies. Here instead, this information will be the basic source data and also an essential tool for the design of the robust controllers. This data will be the clue to define which is the BW we need to attenuate in order to asses the aim of this work. To determine the spectrum of this noise for each velocity two experiments were performed: 1) in a wind tunnel and 2) on a car driving along the freeway. These will be described in Sections III-A and III-B, respectively.

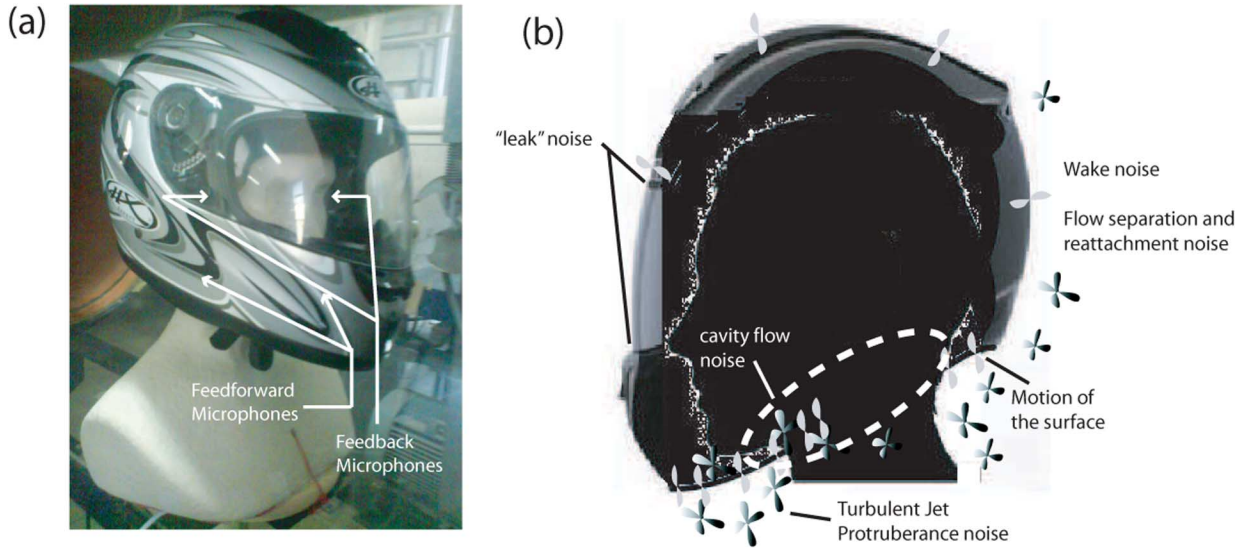

Fig. 1. (a) Helmet and mannikin used in the experiments, the mannikin has a pair of omnidirectional matched microphones in her ears (error microphones) and another pair in the chin bars of the driver (reference microphones). (b) Scheme of the aeroacoustic noise sources for the helmet noise control problem.

B. Control Structure

In [10], [13], and [26], a comparison between three basic control structures [FF, FB and hybrid (FB/FF)] for $\mathcal{H}_\infty$ controllers in ANC applications is performed. This analysis concludes that, in general, the hybrid structure provides maximum performance. Another important conclusion of these works is that a strong performance limitation in the FB design is due to the non-minimum-phase zeros [7]–[9], usually related to time delays. Hence, another reason to include the use of FF is because this limitation is not present.

Here, the signal from the reference microphones is used in the feedforward action, and the error signal and the air velocity are the inputs to the feedback action. The reference microphones are placed in the chin bars of the motorcyclist[2] and the error microphones near the ears. In both cases, matched pairs are selected in order to have similar open circuit sensitivity, frequency, and phase response characteristics. Therefore a symmetric location of sensors and actuators is used, although here for practical reasons, only one side is analyzed. The velocity sensor is placed on the helmet so that no extra noise sources are added. A convenient location could be the top of the helmet.

The three parts of the control structure can be seen in Fig. 2.

- ***Noise Direct Path Identification:*** The noise that affects the ear of the motorcyclist should be predicted and used in the feedforward path. To this end, an identification of the transfer function between the reference and the error microphones should be made.
- ***Feedforward Controller:*** The noise prediction will be used as the input to the FF controller, which is not subject to the feedback loop limitations and has been designed considering the uncertainty on the noise prediction [20].
- ***Feedback Controller:*** The information provided by the feedback (error) microphones will be the input to the LTI FB controller, and in addition the anemometer output will also feed the feedback LPV controller. Both robust controllers will guarantee robust stability and performance of the closed loop [22]–[24], [27], [28]. Furthermore, the fact that the noise spectrum changes (in magnitude and bandwidth) with the relative velocity $v(t)$ is applied as a velocity varying performance weight $W_{fb}(v)$ and used in the design of the FB LPV control. This *tuning* of the performance with air speed $v(t)$ produces a better attenuation than if a single LTI weight $W_{fb}(s)$ is used for all velocities, as in the LTI FB design.

[2]The location of the reference microphones should be studied in more detail in the future as it is a key aspect to obtain better performance. The chin bar of the driver is a good choice because it is close to the main noise source.

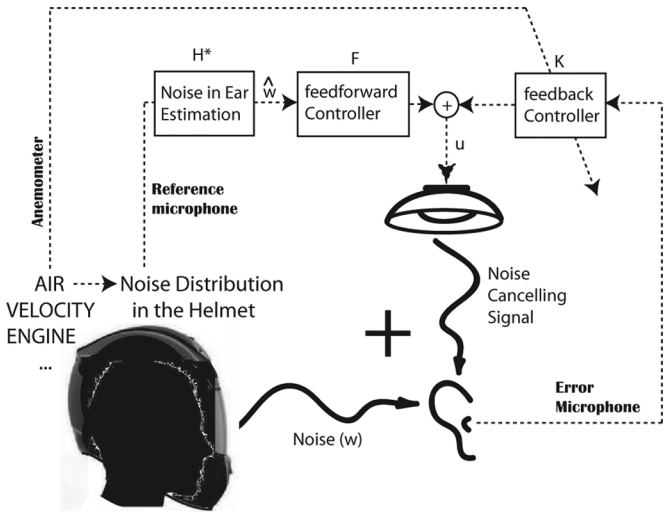

Fig. 2. Scheme of the hybrid control configuration and all the sensors and controllers involved in the control design.

The way to introduce the noise cancelling signal in both, the FB and FF controllers, is through the earphones. Hence, the model of the earphones and its level of uncertainty have to be taken into account in both designs. The earphones and the error microphone have been modelled separating the electrical, mechanical and acoustical parts (see details in [19] and references

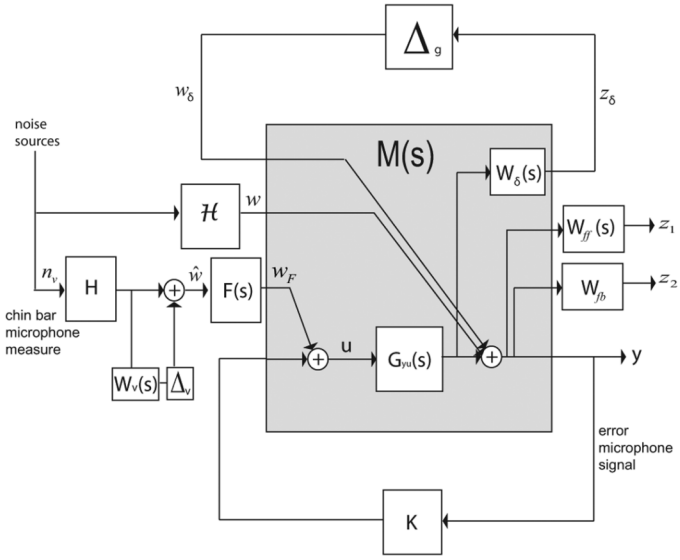

Fig. 3. Control configuration with the FB and FF controllers for both, the LTI and LPV cases.

therein). The transfer function between the voltage input of the speaker and the voltage output of the error microphone, G_{yu} has been obtained as in [16] and [19]. Here, the dynamics are as follows: *electrical impedance:* $Z_e(s) = L_0 s + R_0$; *mechanical impedance:* $Z_m(s) = Ms^2 + R_{ms}s + K/s$; and *acoustical impedance:* $Z_a(s) = C(r)s/s + 2\pi b$. The electrical part includes L_0 which is the inductance of the voice coil and the electrical resistance (R_0). The mechanical one includes the speaker moving mass (M) and the mechanical damping (R_{ms}) and stiffness (K). Finally, the acoustical part has the parameters that explain how the motion of the speaker is translated into air pressure variations. In this part, $C(r) = \rho c/r$ is the microphone dynamics and $b = c/2\pi r'$ is the corner frequency, r is the distance between the earphone and the microphone and r' is the earphone radius. The microphone transfer function is flat from 20 Hz to 20 kHz, and can be modelled by a constant. The uncertainty level for this model has been taken into account in the controller designs [16], [19]. Therefore, the transfer function relating the input voltage of the speaker $V_{\text{in}}(s)$, and the pressure in the ear of the motorcyclist $P(s)$ is defined as follows:

$$G_{yu}(s) = -B\ell \times \frac{AZ_a(s)}{Z_e(s)\left[Z_m(s) + A^2 Z_a(s)\right] + B\ell^2} \tag{1}$$

where $B\ell$ is defined as the voice coil force factor.

According to the controller structure selected, five sensors are needed: one pair of matched omnidirectional (error) microphones located near the ears of the driver, another pair of (reference) microphones next to the chin bar, both for the LTI feedback and feedforward designs, respectively. In addition an anemometer (in the freeway experience) or a pitot tube (in the wind tunnel) to measure relative motorcycle-air velocity for the feedback LPV controller where also used.

The control structure chosen to solve this problem is illustrated by Fig. 3. There were several 2DOF structures that could have been chosen to solve this problem and they were studied in a previous work [19], but the control structure presented in this article offers several advantages. Let us define as the actual transfer function between the chin bar noise (n_v) and the ear noise (w) as $\mathcal{H}$, and its nominal model as $H(s)$. The FF controller is represented by $F(s)$ and the FB controller as K.[3] The uncertainty of the earphone model is represented by Δ_g and the uncertainty in the prediction of the noise in the ear is defined as Δ_v. Note that $W_{ff}(s)$ and $W_{fb}(s)$ (or W_{fb} in the LPV design) are used as performance weights and $W_\delta(s)$ is a robustness weight. $W_v(s)$ can be interpreted as the level of uncertainty in the prediction of the noise in the ear and it works exactly as a performance weight that can be included in W_{ff}. Notice that if no active noise control is used, the actual noise in the ear would be $y = w$.

It is clear that this control structure can also be defined in a normalized way as follows:

$$\begin{bmatrix} z_\delta \\ z_1 \\ z_2 \\ y \end{bmatrix} = \begin{bmatrix} 0 & 0 & W_\delta G_{yu} \\ W_{ff} & W_{ff} & W_{ff}G_{yu} \\ W_{fb} & W_{fb} & W_{fb}G_{yu} \\ 1 & 1 & G_{yu} \end{bmatrix} \begin{bmatrix} w_\delta \\ w \\ u \end{bmatrix} \tag{2}$$

where u is the control input and y is the actual noise in the ear of the driver. Note that the control action is $u = F\hat{w} + Ky$, hence if $\hat{w} = (1 + W_v\Delta_v)w$ and the uncertainty of the system is added, the closed-loop relation between disturbance and performance is

$$T_{z_1 w,ff} = W_{ff}\left[1 + G_{yu}(1 + W_\delta\Delta_g)F(1 + W_v\Delta_v)\right] \tag{3}$$

$$T_{z_2 w,fb} = \frac{W_{fb}}{1 + G_{yu}(1 + W_\delta\Delta_g)K}. \tag{4}$$

Here, $T_{z_1 w,ff}(s)$ has been computed only for the feedforward case $(K \equiv 0)$, and $T_{z_2 w,fb}(s)$ for the feedback case $(F \equiv 0)$. Hence, the resulting transfer function when the hybrid controller is in place, is as follows:

$$T_{yw} = \underbrace{\left[1 + G_{yu}(1 + W_\delta\Delta_g)F(1 + W_v\Delta_v)\right]}_{(I)} \times \underbrace{\frac{1}{1 + G_{yu}(1 + W_\delta\Delta_g)K}}_{(II)}. \tag{5}$$

Note that the feedback and the feedforward noise attenuations (in decibels) will have an additive effect. The FF controller is inversion-based, hence in the nominal case, i.e., no uncertainty, $F(s) \approx -G_{yu}^{-1}(s)$. In addition, for an $\mathcal{H}_\infty$ FB controller, the product $G_{yu}(s)K(s)$ will be large in the BW where the performance is needed. This produces the desired result on both terms $(I) \to 0$ and $(II) \to 0$, for the hybrid controller in the nominal case.

III. Identification of the LPV Noise Spectrum

The purpose of this section is to determine experimentally the spectrum and magnitude of the noise in the helmet due to the external velocity induced noise. This information will be used in the design of the FB and FF controllers to increase performance in the BW where the noise levels are higher, based on the relation between spectrum and relative air velocity. There are previous works related to this issue [3], [14], [25], where the max-

[3] $K(s)$ in the LTI case and $K[v(t)]$ in the LPV design.

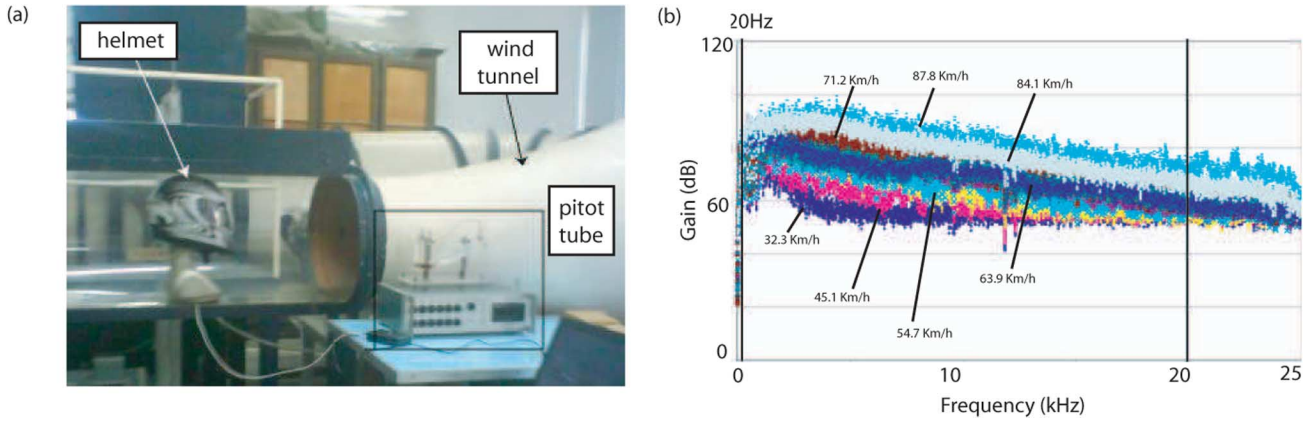

Fig. 4. (a) Experimental setup for the wind tunnel experiment. (b) Noise spectra for different values of the air velocity in the wind tunnel experiment.

Fig. 5. Experimental setup for the freeway experience. The mannikin and the helmet with the microphones and the anemometer were located in the car's roof.

imum level of noise for a certain velocity and for a given helmet can be found, but no one determines the frequency spectrum.

Here, the motorcycle is assumed to have a low windscreen or no windscreen at all, so that the turbulence is directed towards the base of the helmet and the driver's neck and shoulders. Higher windscreens direct the turbulent flow towards the face and, depending upon screen height, hit the visor or the helmet shell immediately above the visor. These alternatives would show different noise patterns and could be studied in a future work.

A. *Wind Tunnel Experiment*

The helmet model chosen for the experiments can be seen in Fig. 1(a). It has been placed on a mannikin because the dominant noise source in the motorcycle helmet is in the base of the helmet, between the chin bar and the neck of the driver [14], [25]. A pair of omnidirectional matched microphones have been placed in the mannikin's ears. The transfer function of these microphones is known and flat in the range $[20, 10000]$ Hz.

The mannikin and helmet were placed inside a wind tunnel (as in [25]). The test chamber for the wind tunnel computes air flow velocity by means of a pitot tube [see Fig. 4(a)] that measures the difference between the atmospheric and air pressures. The wind tunnel [see Fig. 4(a)] used in the experiments is located in the Fluid Mechanics Department in ETSEIB (UPC). It is a metallic subsonic tunnel with a closed circuit, low turbulence level and low velocity. The air flow is generated by a ventilator with guideline propellers, powered by an oleohydraulic pump-engine. With this setup, the sound spectrum in the ear of the motorcyclist was computed for several values of velocity in the rank allowed by the wind tunnel. These results can be seen in Fig. 4(b).

B. *Freeway Experiment*

The mannikin (with the microphones), the helmet and the anemometer with its corresponding transmitter were placed on a car's roof (see Fig. 5). This was done carefully, in order not to generate extra sources of turbulent flow. The anemometer was fixed in a convenient place so that the actual air velocity whose main component is the car velocity, could be determined. For a future industrial design, the location of the anemometer should be studied in order to determine a good measure of the noise BW that is affecting the motorcycle driver. Initially, the top of the helmet shell seems a good choice. The velocity sensor is a 16 mm diameter vane measurement probe, with temperature and velocity ranges of $[0, 60]$°C and $[0.6, 40]$ m/s($[2{,}144]$ km/h), respectively. The car battery was used to power the anemometer and all the data was collected with a portable oscilloscope. The experiment was performed at velocities ranging from 20 to 120 km/h in a freeway. The data obtained from the experiment can be seen in Figs. 6 and 7.

C. *Discussion*

In both experiments, the fact that the noise in the ear increases with the velocity is clear. The noise pressure levels from the first experiment were not useful due to the high environmental noise

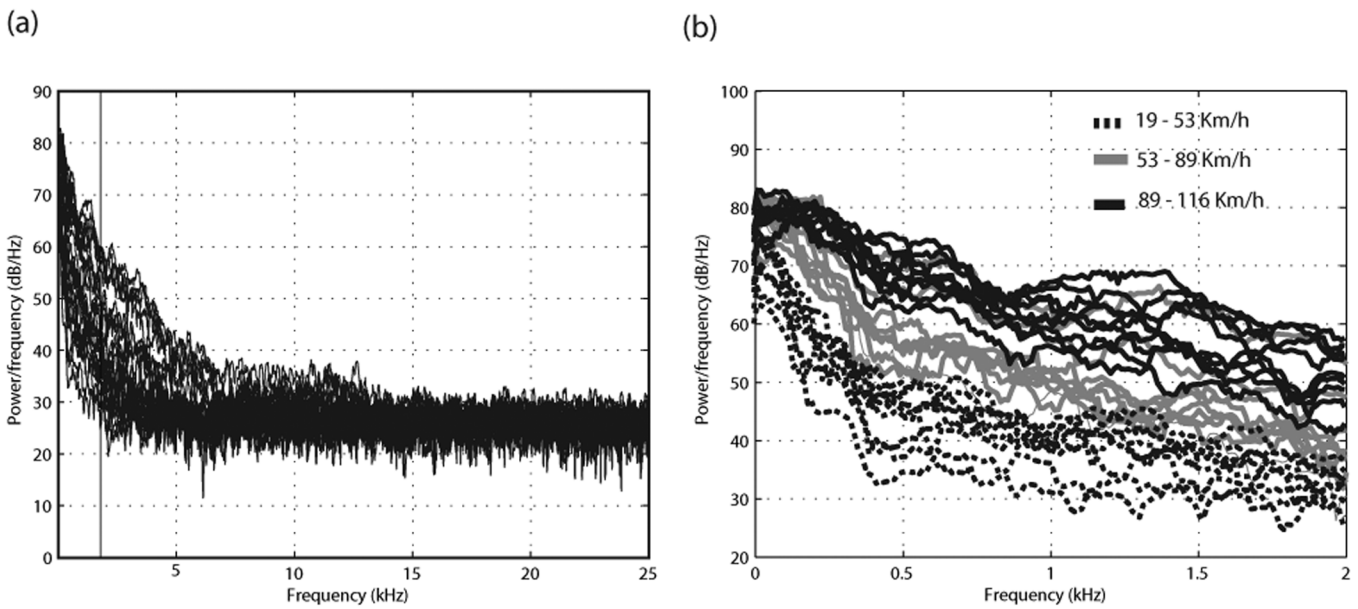

Fig. 6. (a) Noise spectra for different values of the car-air velocity in the freeway experiment estimated via Thompson Multitaper and (b) detail of the most annoying BW.

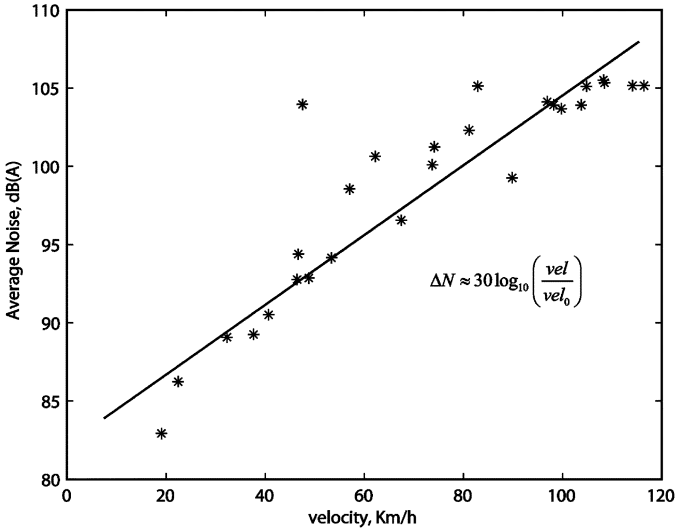

Fig. 7. Average noise as a function of car-air velocities in the freeway experiment.

caused by the tunnel fan and the vibration of the methacrylate chamber. In Fig. 7 the noise pressure levels for the second experiment can be seen. Note that the noise in the ear of the driver increases linearly with the $\log_{10}$ of the velocity. The relation is approximately the following $\Delta N \approx 30 \log_{10} v/v_0$.

Here ΔN is the increment of noise [in decibels(A)], v is the air velocity and v_0 is the reference air velocity. This data is fully consistent with the works in [3] and [5] where the sound pressure levels where computed for different types of helmets and a wide range of air velocities.

It is known that the efficiency of the FB controller is limited by the characteristics of the loop. Instead, the efficiency of the FF controller is only limited by the knowledge of the transfer functions between (a) the chin bar noise and the noise in the ear and (b) the earphones (with a BW of [18,22000] Hz, and its level of uncertainty. For these reasons, the bandwidth where the attenuation is needed has to be carefully chosen in order for both controllers to provide the best attenuation. In Fig. 6, the most perturbing frequencies can be seen to lie in the range [20,1500] Hz. This figure has been used to design the performance weights in both, the LTI and LPV controller designs. In the latter, the magnitude and frequency response of this weight changes with the air velocity, which should be measured in real time.

IV. Designs and Results

A. LTI Controller Design

The robust performance feedforward problem to be solved is the following:

$$\sup_{\bar{\sigma}(\Delta)<1} \left\| F_u\left(M_{ff}, \Delta\right) \begin{bmatrix} I \\ F \end{bmatrix} \right\|_{i2} < \gamma \tag{6}$$

where $F_{u(\ell)}$ is the upper (lower) linear fractional transformation, $\|\cdot\|_{i2}$ denotes the $\mathcal{L}_2$ induced norm, $\Delta = \text{ diag}\left(\Delta_v, \Delta_g\right)$ and $M_{ff}(s)$ is defined as

$$\begin{bmatrix} z_{vel} \\ z_\delta \\ z_1 \end{bmatrix} = \underbrace{\begin{bmatrix} 0 & 0 & 0 & W_v \\ W_\delta G_{yu} & 0 & 0 & W_\delta G_{yu} \\ W_{ff} G_{yu} & W_{ff} & W_{ff} & W_{ff} G_{yu} \end{bmatrix}}_{M_{ff}} \begin{bmatrix} w_{vel} \\ w_\delta \\ w \\ w_F \end{bmatrix}. \tag{7}$$

Here we have switched F with the multiplicative uncertainty blocks (W_v, Δ_v) in Fig. 3, due to the fact that the system is SISO. This controller [see Fig. 8(a)] has been designed via robust (weighted) $\mathcal{H}_\infty$ synthesis [20], [29], [30]. Using the results in [20], the infinite dimensional problem is reduced to a finite

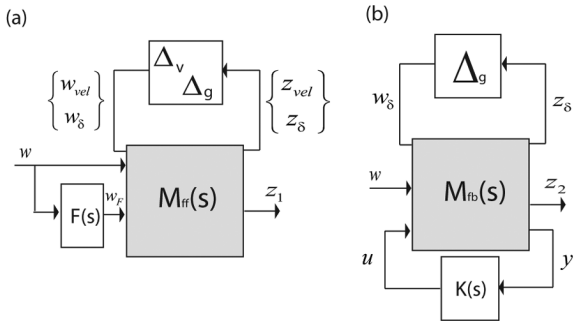

Fig. 8. Control configuration scheme for the (a) feedforward and the (b) feedback LTI controllers.

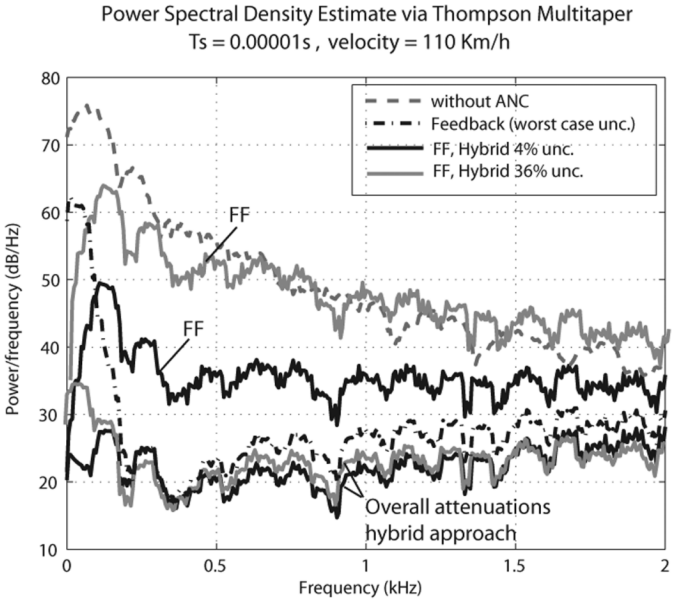

Fig. 9. Spectrum of the air pressure levels for different configurations and different levels of uncertainty in the estimation of $\dot{w}$ for a fixed velocity.

dimensional one by restricting the frequency dependent functions of the uncertainty set to rational transfer functions with fixed order and denominator, i.e., $N(\jmath\omega)/d(\jmath\omega) \cdot d(\jmath\omega)$. Here $d(s) = s^2 + 1960s + 2.6 \times 10^6$, and the resulting feedforward controller has order 11. Another option could be the use of an adaptive identification/cancellation scheme, which has as its main disadvantage the possible instability at implementation [21]. Here, a comparison between several adaptive schemes (RLS, LMS, normalized LMS, sign-sign LMS, sign-error LMS) and the LTI FF algorithm has been performed. A thorough comparison between both methodologies will be the object of future research.

The FB controller [see Fig. 8(b)] is designed via a standard discrete $\mathcal{H}_\infty$ LMI approach with $M_{fb}(s)$ defined as follows:

$$\begin{bmatrix} z_\delta \\ z_2 \\ y \end{bmatrix} = \underbrace{\begin{bmatrix} 0 & 0 & W_\delta G_{yu} \\ W_{fb} & W_{fb} & W_{fb} G_{yu} \\ 1 & 1 & G_{yu} \end{bmatrix}}_{M_{fb}} \begin{bmatrix} w_\delta \\ w \\ u \end{bmatrix}. \tag{8}$$

The resulting FB controller has order 9. The weights indicated in Fig. 3 have been selected as follows:

$$W_{ff}(s) = 0.8\ \frac{(s+10^5)(s+0.00025)}{s^2+502.7s+3.9\cdot 10^5} \tag{9}$$

$$W_{fb}(s) = \frac{9.92\cdot 10^6\ s^2}{s^2+502.7s+3.9\cdot 10^5} \tag{10}$$

$$W_\delta(s) = \frac{16(s+10^4)}{s+10^6}. \tag{11}$$

The two controllers have been discretized with a sampling period that has been chosen to be 0.01 ms. This is due to the fact that both, the feedforward [20] and LPV design methods tend to produce fast poles. In the first case, there is no direct discrete time design method, and in the latter case this problem can be mitigated by means of an extra pole placement LMI (see [31] and [32]), probably at the expense of some performance loss. Nevertheless, from the implementation point of view, the hybrid LTI and LPV controllers have similar complexity. In the latter case, only the $v(t)$ signal should be added to the hybrid structure to schedule the FB time varying control. The order of the FB and the FF controller are 8th and 9th, respectively. Therefore, the DSP has to compute 34 sums and 34 products to obtain the voltage input to the headphones. DSPs are developed to efficiently compute the multiply-and-accumulate unit (MAC). For example the TI C64x architecture can compute 4 product/adds in one cycle, so the execution of the hybrid LPV controller would take around 9 clock cycles. Recent DSPs have a clock frequency of 600 MHz, so the computation time for the hybrid controller would be 15 ns, and the acquisition time for the most recent AD/DA Converters is around 5.5 μs (resolutions of 24 bits). Therefore, with the actual sampling time (0.01 ms), the implementation is feasible. Experience with older versions of DSPs applied to ANC in tubes have been performed in our group with sampling times of 0.2 ms.

The design seeks to achieve the best level of performance in the range where the highest levels of noise pressure are detected, i.e., from 20 to 1500 Hz. Two simulations have been performed using the experimental data from the freeway test, one for fixed and the other for variable velocities.

1) Constant Velocity Robust Performance Test: The first experiment consisted on evaluating the performance of the system for different values of uncertainty in the ear noise estimation, at a constant speed. The results are presented in Table I, Figs. 9, and 13(a). The level of uncertainty depends on the location of the reference microphones, which have been placed in the driver's chin bars, according to a preliminary study of the helmet aeroacoustics. In Table I and Fig. 13(a), the results of the attenuation for different values of uncertainty are presented.

The feedback attenuation is the same for all cases, because the worst case feedback uncertainty has been taken into account in the design, and the air velocity is fixed. Instead, the feedforward attenuation increases from -6.3 dB up to -21.5 dB when the uncertainty of the ear noise estimation decreases from 48% to 4%. The results for the hybrid configuration show that actual noise attenuation levels are similar for uncertainties ranging from 0% to 36%, and for higher uncertainty levels the performance slightly decreases. As a conclusion, the addition of a FF controller to the classical feedback one improves the resulting performance even for high uncertainty levels. From the

TABLE I
NOISE ATTENUATION AT 110 KM/H (ALL IN DECIBELS)

Uncertainty	FB	FF	Hybrid
4%	-16	-21.5	-21.9
8%	-16	-19.2	-22.4
12.5%	-16	-17	-23.3
16%	-16	-15.2	-22.5
25%	-16	-12.4	-23.1
32%	-16	-10.5	-23
36%	-16	-9.6	-22.8
44%	-16	-8	-20.7
48%	-16	-6.3	-19.2

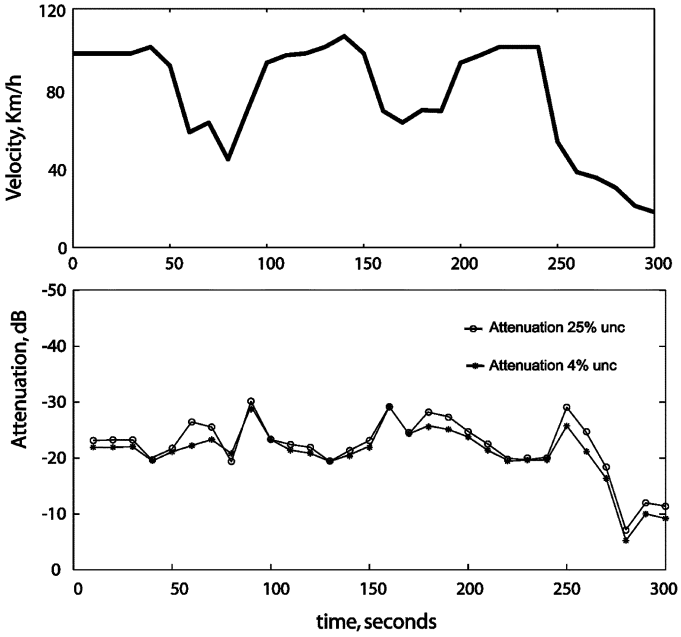

Fig. 10. Noise attenuation versus variations on the air velocity.

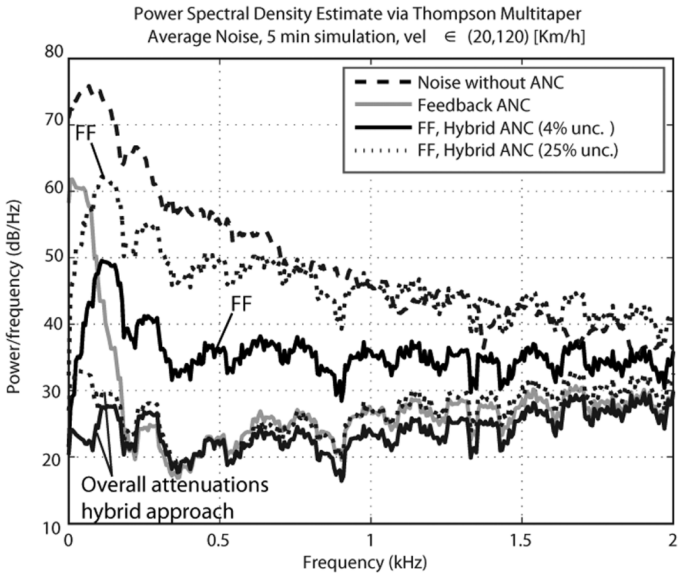

Fig. 11. Spectrum of the air pressure levels for different configurations and different levels of uncertainty in the estimation of $\hat{w}$.

TABLE II
NOISE ATTENUATION DURING THE JOURNEY (ALL IN DECIBELS)

Uncertainty	FB	FF	Hybrid
4%	-17.6	-19.4	-21.1
25%	-17.6	-10.7	-22

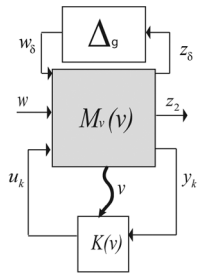

Fig. 12. Design of the LPV FB controller.

frequency point of view, Fig. 9 illustrates that the FF controller is highly effective at lower frequencies, while the attenuation levels in $[300, 1000]$ Hz are mainly due to the FB controller. Note that in the bandwidth between 250 to 1500 Hz, the FF controller increases significantly the attenuation as uncertainty in $H(s)$ decreases. Nevertheless this improvement is not as significant when combined with the FB controller.

2) Varying Velocity Test: Here, the behavior of the LTI hybrid controller under noise spectrum changes due to velocity variations, has been tested. Again, the noise/velocity time series collected during the freeway experiment (from 20 to 117 km/h) where used. This data has been rearranged in a simulated 5 min journey, to study the noise attenuation performance of the system. In the upper plot of Fig. 10, the velocity profile is presented.

The simulation has also tested feedforward uncertainty levels of 4% and 25%, combined with the worst case uncertainty in the feedback loop. The results are presented in Figs. 10 and 11. The attenuations for both values of uncertainty are very close and the average noise for the complete journey is decreased in approximately 21 dB.

The results for the feedback, the feedforward, and the hybrid configuration can be seen in Table II separately. The first column indicates the uncertainty level in the chin bar microphones, the second and third columns present the attenuation for the feedback and the feedforward configurations separately, and finally, the forth column present the actual attenuation for the hybrid configuration. As in the previous experiment, the worst case uncertainty for the FB controller has been taken into account in all the cases.

B. Time Varying Controller Design

Here, the spectrum and noise pressure changes with velocity illustrated in Fig. 6, where used to design the FB controller. The design seeks the maximum level of performance for a range of frequencies *tuned* with the actual velocity. To this end, the performance weight for the feedback design is adjusted in order to obtain maximum performance at each velocity. Take for example in the same figure, for low velocities ($\leq$ 60 km/h) the most disturbing frequencies are in the 20–500 Hz frequency

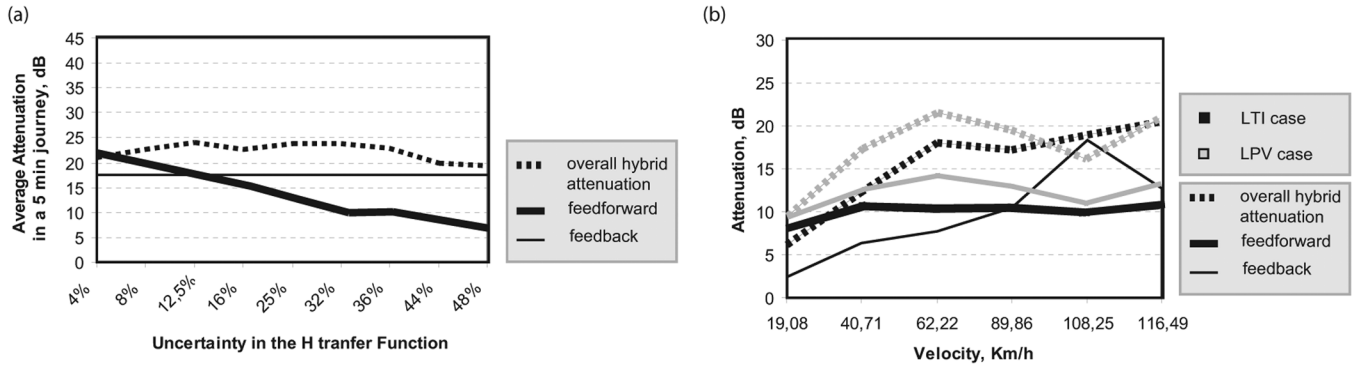

Fig. 13. (a) LTI overall attenuation for different values of uncertainty in the FF path, worst case uncertainty in the FB path. (b) Theoretical and Real Attenuation for the Hybrid Control Configuration in the LTI and LPV cases.

band. Hence, it is possible to improve the overall performance with a parameter varying controller scheduled by the relative motorcycle-air velocity.

The control structure for the design of the linear parameter varying FB controller can be seen in Fig. 3, which can be transformed into Fig. 12. In the first figure, the performance weight W_{fb} and the controller K are both LPV models, the latter designed according to [27]. Here $v(t)$ is the air velocity measured by the anemometer and the varying FB controller is adapted according to this value. The LTI uncertainty in the earphone model is Δ_g, and M_v is the LPV augmented model of the system. According to standard results, the controller guarantees closed-loop internal stability for all parameter trajectories $\mathcal{P} = \{v(t) \in [0{,}120]\}$, and performance based on the induced $\mathcal{L}_2$-norm of the closed-loop system

$$\max_{K_{stabilizing}} ||F_\ell \left[M_v(v), K(v)\right]||_{i2} < \gamma. \qquad (12)$$

By defining $\varsigma = \begin{bmatrix} z_\delta \\ z_2 \end{bmatrix}$ and $\varrho = \begin{bmatrix} w_\delta \\ w \end{bmatrix}$, the system in Fig. 12 (without the controller) can be represented as follows:

$$\begin{bmatrix} \dot{x} \\ \varsigma \\ y_k \end{bmatrix} = \begin{bmatrix} A(v) & B_1 & B_2 \\ C_1(v) & D_{11} & D_{12} \\ C_2 & D_{21} & D_{22} \end{bmatrix} \begin{bmatrix} x \\ \varrho \\ u_k \end{bmatrix}. \qquad (13)$$

This corresponds to the state space representation of (8), but with a time-varying W_{fb} which depends on $v(t)$.

One of the assumptions in this approach is that $B_2(v), C_2(v)$, $D_{12}(v)$, $D_{21}(v)$ are parameter-independent, which is the case for this system. However for a more general time varying model it can be solved with a post-filter in the control inputs u and a prefilter in the measured outputs y (see [28]). The model is affine in the parameter $v(t)$, therefore the design LMIs only need to be solved at the extremes of the velocity interval to compute the LPV controller. The LPV controller state space representation is $S_K = \{S_0 \left[v(t) - v_1\right] + S_1 \left[v_0 - v(t)\right]\} / (v_0 - v_1) = \begin{bmatrix} A_k(t) & B_k(t) \\ C_k(t) & D_k(t) \end{bmatrix}$. Its value for the slower velocity v_0 is S_0 and the controller for the faster velocity v_1 is S_1.

1) Results: The LPV feedback and LTI FF controllers have been tested considering a 48% of uncertainty in the estimation of $\hat{w}$ in Fig. 3 as well as worst case uncertainty in the FB loop. The performance results for this hybrid time varying control system are presented in Table III. These results are also illustrated in Fig. 13 where the noise pressure attenuations for different air velocities are plotted. Note that the LPV approach allows more performance for a fixed controller order, specially when the air velocities are low (< 90 km/h). This is due to the fact that the BW of the input signal is narrower.

TABLE III
FB, FF, NORMALIZED-LMS AND HYBRID LTI AND LPV ATTENUATION RESULTS (ALL IN DECIBELS)

V (Km/h)	FB (LTI)	FB (LPV)	FF	Norm LMS	Hyb (LTI)	Hyb (LPV)
19.1	-2.5	-9.4	-8.1	0.049	-6	-9.3
40.7	-6.3	-12.6	-10.6	0.0011	-13.5	-16.3
62.2	-7.7	-14.1	-10.3	0.0029	-18.4	-21.9
89.9	-10.4	-12.9	-10.4	-0.0055	-17.1	-18.6
108.3	-15.4	-10.9	-9.9	-0.0305	-17.7	-16.4
116.5	-12.8	-13.1	-10.7	-0.0227	-19.5	-19.5

Also note that in Fig. 13(a), the results indicate that for lower values of uncertainty in $H(s)$ ($\leq 36\%$), the attenuation could be improved in 2–3 dB even at high air speeds. Recall that for these velocities, the noise level is higher too.

Overall, from the results presented in these plots and in Table III, it is clear that the use of the LPV hybrid approach performs up to 4 dB better (in average) than the LTI hybrid controller. In addition, Fig. 14 shows that using the hybrid LPV ANC system, the noise in work legislation can be accomplished even when taking into account the worst case uncertainty in the FB controller and 48% uncertainty in the feedforward action.

Several adaptive filters (RLS, LMS, normalized LMS, sign-sign LMS, sign-error LMS) have also been tested for the FF path. However, the results obtained with all of them has been poor or even unstable (LMS) for the current application. The best attenuations have been obtained using the normalized LMS algorithm and they are presented in Table III. Performance results for the RLS algorithm are similar. In the future, a thorough comparison with other robust adaptive procedures, e.g., σ-modified, projection algorithm [21], will be performed.

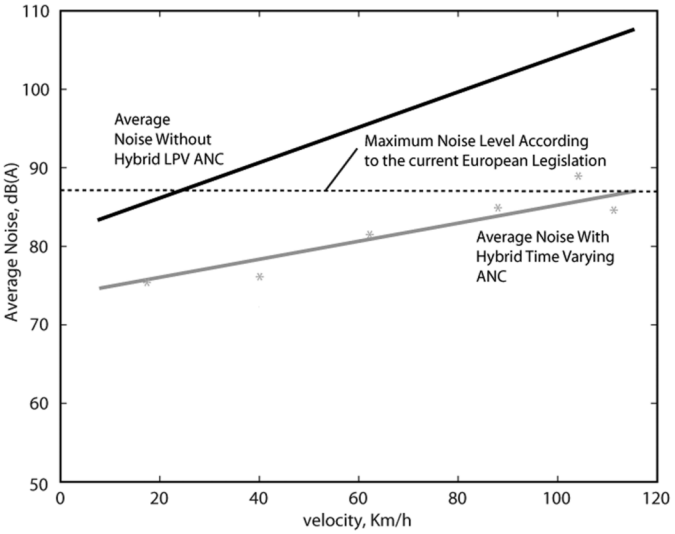

Fig. 14. Average noise attenuation versus air velocity. The grey line presents the results when the worst case uncertainty is applied to the feedback controller and there is a 48% of uncertainty in the prediction of the noise in the ear.

V. Conclusion and Future Research

This motivating preliminary study produces two hybrid (FF + FB) controllers which are applied to the problem of ANC in motorcycle helmets. The first one is a combination of LTI FB and FF controllers, the second is the same LTI FF combined with a time varying LPV FB controller. Both FF controllers use as an input signal the measurement of the aerodynamic external noise in the helmet chin bar. The LPV scheduling parameters is the velocity $v(t)$ measured in real time by an anemometer.

The simulation results based on real experimental data and physical models of the helmet system, show that the ANC hybrid LPV control structure seems promising for future controller tests to be performed in real time. This controller satisfies the recent European Legislation for motorcycle helmet noise attenuation, which protects the auditive health of occupational motorcycle drivers, even with high levels of uncertainty.

Future work includes a real time experimental test of the hybrid LPV controller and an LTI or LPV identification of the FF path, including the possibility of implementing an adaptive identifier. In addition, the best location of the reference microphones should be studied carefully. Recall that the performance achieved by the FF controller is highly dependent on the uncertainty in the prediction of the noise in the ear, which in turn is directly related to the location of these microphones. The selection of the time scheduling sensor is another practical issue: anemometer, pressure sensor or accelerometers (with lower manufacturing costs).

Acknowledgment

The authors would like to thank Prof. M. Brennan and the Institute of Noise and Vibration Research (ISVR, Southampton, U.K.) for their helpful comments and valuable suggestions. At UPC, they appreciate the essential help provided by the Fluid Dynamics Department (Barcelona) personnel for allowing them to perform the wind tunnel experiment, as well as to the Department of Electronics (Terrassa).

References

[1] Official Journal of the European Community, "Directive 2003/10/EC, noise at work regulations," UE-2003/10/EC, 2003.
[2] W. V. Moorhem, K. Sheperd, T. Magleby, and G. Torian, "The effects of motorcycle helmets on hearing and the detection of warning signals," *J. Sound Vibr.*, vol. 8, pp. 30–2, 1981.
[3] A. W. McCombe, J. Binnington, and D. Nash, "Two solutions to the problem of noise exposure for motorcyclists," *Occupational Med.*, vol. 44, pp. 239–242, 1994.
[4] A. W. McCombe, "Hearing loss in motorcyclists: Occupational and medicolegal aspects," *J. Royal Soc. Med.*, vol. 96, pp. 7–9, 2003.
[5] C. Jordan, "Noise induced hearing loss in occupational motorcyclists," *J. Environmental Health Res.*, vol. 3, pp. 373–382, 2004.
[6] J. J. Lazzeroni and M. K. Carevich, "Noise cancelling microphone for full coverage style helmets," U.S. Patent 5 684 880, Nov. 4, 1997.
[7] M. Seron, J. Braslavsky, and G. Goodwin, *Fundamental Limitations in Filtering and Control*. New York: Springer, 1997.
[8] J. Hong and D. Bernstein, "Bode integral constraints, colocation, and spillover in active noise and vibration control," *IEEE Trans. Control Syst. Technol.*, vol. 6, no. 1, pp. 111–120, Jan. 1998.
[9] J. Freudenberg, C. Hollot, R. Middleton, and V. Toochinda, "Fundamental design limitations of the general control configuration," *IEEE Trans. Autom. Control*, vol. 48, no. 8, pp. 1355–70, Aug. 2003.
[10] S. Kuo and D. Morgan, *Active Noise Control Systems: Algorithms and DSP Implementations*. New York: Wiley, 1995.
[11] P. Nelson and S. Elliot, *Active Control of Sound*. New York: Academic Press, 1992.
[12] M. Bai and H. Lin, "Plant uncertainty analysis in a duct active noise control problem by using the $\mathcal{H}_\infty$ theory," *J. Acoust. Soc. Amer.*, vol. 104, no. 1, pp. 237–247, Jul. 1998.
[13] R. S. Sánchez Peña, J. Quevedo, and V. E. Puig, *Identification and Control: The Gap Between Theory and Practice*. London, U.K.: Springer-Verlag, 2007, ch. Identification and Control Structure Design in Active (acoustic) Noise Control, pp. 203–244.
[14] R. Pääkkönen and P. Kuronen, "Noise attenuation of helmets and headsets used by finnish air force pilots," *Appl. Acoust.*, vol. 49, pp. 373–382, 1996.
[15] W. S. Gan, S. Mitri, and S. M. Kuo, "Adaptive feedback active noise control headset: Implementation, evaluation and its extensions," *IEEE Trans. Consumer Electron.*, vol. 51, no. 3, pp. 975–982, Aug. 2005.
[16] A. D. White, "On loudspeaker implementation for feedback control, open-air, active noise reduction headsets," M.S. thesis, Mech. Eng. Dept., Virginia Polytechnic Institute and State University, Blacksburg, 1999.
[17] B. Rafaely and S. Elliot, "H_2/H_∞ active control of sound in a headrest: Design and implementation," *IEEE Trans. Control Syst. Technol.*, vol. 7, no. 1, pp. 79–84, Jan. 1999.
[18] S. M. Kuo, S. Mitra, and W.-S. Gan, "Active noise control system for headphone applications," *IEEE Trans. Control Syst. Technol.*, vol. 14, no. 2, pp. 331–335, Mar. 2006.
[19] R. Castañé and R. S. Peña, "Control activo de ruido acústico en cascos de motociclismo," *Revista Iberoamericana de Automática e Informática Industrial*, vol. 4, no. 3, pp. 73–85, 2007.
[20] G. Scorletti and V. Fromion, "Further results on the design of robust $\mathcal{H}_\infty$ feedforward controllers and filters," in *Proc. Conf. Dec. Control*, 2006, pp. 3560–3565.
[21] R. Ortega and Y. Tang, "Robustness of adaptive controllers-a survey," *Automatica*, vol. 25, no. 5, pp. 651–77, 1989.
[22] K. Zhou, J. C. Doyle, and K. Glover, *Feedback Control Theory*. Englewood Cliffs, NJ: Prentice-Hall, 1996.
[23] R. S. Sánchez Peña and M. Sznaier, *Robust Systems Theory and Applications*. New York: Wiley, 1998.
[24] J. Doyle and A. T. B. Francis, *Feedback Control Theory*. New York: Macmillan, 1990.
[25] M. Lower, D. Hurst, A. Claughton, and A. Thomas, "Sources and levels of noise under motorcyclists' helmets," in *Proc. Inst. Acoust.*, 1994, pp. 319–326.
[26] M. Bai and D. Lee, "Comparison of active noise control structures in the presence of acoustical feedback by using the $\mathcal{H}_\infty$ synthesis technique," *J. Sound Vibr.*, vol. 206, no. 4, pp. 453–471, 1997.
[27] P. Gahinet and P. Apkarian, "A convex characterization of gain-scheduled $\mathcal{H}_\infty$ controllers," *IEEE Trans. Autom. Control*, vol. 40, no. 5, pp. 853–864, May 1995.
[28] P. Apkarian, P. Gahinet, and G. Becker, "Self-scheduled $\mathcal{H}_\infty$ control of linear parameter-varying systems: A design example," *Automatica*, vol. 31, no. 9, pp. 1251–1261, 1995.
[29] A. Giusto and F. Paganini, "Robust synthesis of feedforward compensators," *IEEE Trans. Autom. Control*, vol. 44, no. 8, pp. 1578–1582, Aug. 1999.

[30] K. Sun and A. Packard, "Robust H_2 and H_∞ filters for uncertaint LFT systems," *IEEE Trans. Autom. Control*, vol. 50, no. 5, pp. 715–720, May 2005.
[31] A. S. Ghersin and R. S. Sánchez Peña, "Transient shaping of LPV systems," in *Proc. Eur. Control Conf. (Invited Paper)*, 2001, pp. 3080–3085.
[32] A. S. Ghersin and R. S. Sánchez Peña, "LPV control of a 6 DOF vehicle," *IEEE Trans. Control Syst. Technol.*, vol. 10, no. 6, pp. 883–887, Nov. 2002.

Rosa Castañé-Selga (S'07) was born in Lluçà, Spain. She received the M.Sc. degree and Diploma of Advanced Studies in Engineering from Universitat Politècnica de Catalunya, Catalunya, Spain, in 2005 and 2008, respectively. She is currently pursuing the Ph.D. degree in automatic control at the Technische Universität München, Munich, Germany, being supported by a research scholarship of the Elite Network of Bavaria.

She has held visiting research positions at the Department of Automatic Control of the Lund Institute of Technology, Lund, Sweden (2005) and at the Institute of Sound and Vibration Research of Southampton University, Southampton, U.K. (2007). Her research interests include systems theory, model order reduction of large scale systems, active noise control of sound and vibration, and robust control and identification.

Ricardo S. Sánchez Peña (SM'00) received the B.S. degree in electronic engineering from the University of Buenos Aires, Buenos Aires, Argentina, in 1978, the M.S. and Ph.D. degrees from California Institute of Technology, Pasadena, in 1986 and 1988, respectively.

He worked in CITEFA (1977–1979), CNEA (1989–1994) and in spacecraft navigation and control in the argentine Space Agencies, CNIE (1979–1984) and CONAE (1994–2004) with collaborations for NASA, DLR (Germany), CTA/INPE (Brazil), and ZonaTech (Phoenix). He was Professor at the University of Buenos Aires (1989–2004), ICREA Research Professor at the UPC, Spain (2005–2009), and visiting Researcher/Professor at Universities in USA and EU. He published 3 books and more than 100 journal and conference papers. Since 2009, he directs the Ph.D. program at the Buenos Aires Institute of Technology as a CONICET Principal Investigator. His research interests include the applications of Robust Identification and Control to practical problems in Engineering.

Dr. Sánchez Peña is a Full Member of the International Academy of Astronautics, Senior Member of AIAA, and Policy Committee member of IFAC (2005–2008).